$\mathbb{Z}_2$ Peak of Noise Correlations in a Quantum Spin Hall Insulator

Jonathan M. Edge,[1] Jian Li,[2] Pierre Delplace,[2] and Markus Büttiker[2]
[1]*Instituut-Lorentz, Universiteit Leiden, P.O. Box 9506, 2300 RA Leiden, The Netherlands*
[2]*Département de Physique Théorique, Université de Genève, CH-1211 Genève, Switzerland*
(Received 9 April 2013; published 10 June 2013)

We investigate the current noise correlations at a quantum point contact in a quantum spin Hall structure, focusing on the effect of a weak magnetic field in the presence of disorder. For the case of two equally biased terminals we discover a robust peak: the noise correlations vanish at $B = 0$ and are negative for $B \neq 0$. We find that the character of this peak is intimately related to the interplay between time reversal symmetry and the helical nature of the edge states and call it the $\mathbb{Z}_2$ peak.

DOI: 10.1103/PhysRevLett.110.246601 PACS numbers: 72.70.+m, 72.10.−d, 73.23.−b, 85.75.−d

Measurements of current noise correlations can offer remarkable new insights beyond conductance measurements [1]. An example of this is the two-particle Aharonov-Bohm effect in which the presence of a flux can only be determined by measuring noise correlations [2,3]. Quantum spin Hall (QSH) systems, discovered [4] after pioneering studies of time reversal invariant band insulators [5,6], are no exception in this regard. So far, various measurements have characterized the QSH effect from several aspects. First, the quantized conductance was measured in a QSH bar [4]. Nonlocal current measurements subsequently showed that the currents are carried via quantized edge modes [7]. The spin polarization of these edge modes was established very recently [8], thereby vindicating the intuitive picture of the QSH effect consisting of two time reversed copies of the quantum Hall effect. Scanning techniques [9–11] have now provided additional insights into, e.g., inelastic scattering in the QSH systems [12].

To investigate current noise in mesoscopic structures, a central element is the quantum point contact (QPC) [13,14]. Theoretical studies of QPCs in QSH systems have shown ways to test the properties of the helical edge states [15–17] and determine interaction strengths of the edge modes [18]. Current noise studies have been performed to distinguish one- and two-particle tunneling processes at the QPC [19]. Correlations between current noises have also been investigated to this end [20], as has the effect of interactions on the noise correlations of the current which is backscattered from a QPC [21]. One question remains open, however, despite its direct experimental relevance: how do the noise correlations vary with a magnetic field that breaks the time reversal symmetry (TRS)? In this scenario, the topologically protected edge states are singular at zero field; otherwise, disorder becomes crucial. This is the question that we address in the present Letter.

We investigate the noise correlations in a Hall-bar structure with a QPC in a QSH system (see Fig. 1). Our investigation is based on scattering theory [22], which assumes the edge modes to be approximately noninteracting channels. Studies of helical Luttinger liquid theories have shown this to be a good approximation for practical QSH systems in the presence of disorder [23,24], magnetic field [25], as well as a QPC [16]. The relevant scattering matrix in the present setup relating contacts 1 to 4 is a four-by-four matrix (contacts 5 and 6 will be kept grounded). We denote the scattering amplitude for an electron coming from contact β and going into contact α to be $S_{\alpha\beta}$. In previous work [26], it has been shown that in the presence of TRS, $S_{\alpha\alpha} = 0$, $S_{13} = -S_{31}$, $S_{24} = -S_{42}$, and $S_{\alpha\beta} = S_{\beta\alpha}$ otherwise. All the off-diagonal entries of S are in general nonzero [27]. An immediate consequence of the vanishing diagonal entries of S is that the equilibrium noise (autocorrelation) at each contact is universal—it is proportional to the number of open channels connected to the contact [22], but has no dependence on the details of the QPC. When TRS is broken, the diagonal entries of S become also nonzero, signifying the onset of backscattering, and the matrix S is only subject to unitarity. Using the scattering theory for coherent quantum transport [22], we can readily write down the noise correlations in terms of the scattering matrix. We will assume in the following the zero-temperature, zero-frequency limit.

We start with the single-source case, namely we set $eV_1 > 0$, $eV_{2,3,4} = 0$, with V_α the voltage at contact α. The cross-correlation noise power is then given by [1,22]

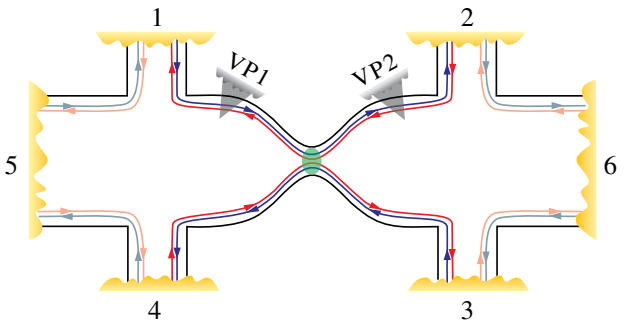

FIG. 1 (color online). Six terminal Hall bar structure with a quantum point contact. VP 1 and VP 2 are voltage probes which allow for inelastic scattering.

$$P_{\alpha\beta} = -\frac{e^2}{h}(eV_1)|S_{\alpha 1}|^2|S_{\beta 1}|^2. \quad (1)$$

This is the partition noise caused by the splitting of the electronic beam at the QPC and it is nonpositive.

Next, we consider the more interesting case of two biased contacts. To be specific, we set $eV_{1,2} = eV_0 > 0$ and $eV_{3,4} = 0$. We will focus on the current cross correlations between the two unbiased contacts (3 and 4). Which two contacts are biased and which are measured is in fact immaterial. In this case, the cross-correlation noise power P_{34} contains not only the partition noise similar to Eq. (1), but also the exchange noise resulting from scattering of two indistinguishable electrons coming from two different contacts. It is given by

$$P_{34} = -\frac{e^2}{h}(eV_0)[|S_{31}|^2|S_{41}|^2 + |S_{32}|^2|S_{42}|^2 + S_{31}^* S_{42}^* S_{32} S_{41} + S_{31} S_{42} S_{32}^* S_{41}^*]. \quad (2)$$

The exchange noise, corresponding to the second line of the above equation, can carry nontrivial information encoded in the phases of the scattering amplitudes and manifest it through two-particle interference [28]. This distinguishes the exchange noise from other measurable quantities to which only scattering *probabilities* are relevant, such as conductance and the pure partition noise.

The total noise power P_{34} is also negative semidefinite, which can be seen by simply rewriting Eq. (2) as $P_{34} = -(e^3 V_0/h)|S_{33}^* S_{43} + S_{34}^* S_{44}|^2$. Here the unitarity of the scattering matrix has been used to equate $|S_{31}^* S_{41} + S_{32}^* S_{42}|$ with $|S_{33}^* S_{43} + S_{34}^* S_{44}|$. One important implication of the above equation is the following: in the presence of TRS, P_{34} reaches its maximum (zero) as $S_{33} = S_{44} = 0$ [29]; when TRS is broken and backscattering sets in, P_{34} generally becomes negative. We call this peak in the current cross correlations the $\mathbb{Z}_2$ peak because it is a peculiar phenomenon associated with the form of the scattering matrix of time-reversal-invariant topological insulators. It is clear that this phenomenon does not depend on the choices of biased or measured contacts, since we have made no special assumption about the contacts so far.

Physically, the $\mathbb{Z}_2$ peak is a result of an exact cancellation between the partition noise and the exchange noise. It is known [1,22] that the partition noise, due to the particle nature of electrons, is negative semidefinite, whereas the exchange noise, due to the fermionic nature of electrons, is positive semidefinite. The two contributions are not necessarily related in generic cases. Here, however, TRS and current conservation together demand that the two contributions be of equal magnitude. Similar cancellations can occur in two other circumstances. In one, both outgoing channels are fully occupied at a specific energy. This happens, for example, in a QPC based on chiral edge states [30,31] where both incoming channels are fully occupied at the same energy. In this case the cancellation is trivial because it merely reflects the absence of current fluctuation in each channel. Similarly, a properly timed mesoscopic two-particle collider with identical sources can lead to a cancellation of the noise correlations [32], as recently demonstrated in an electronic on-chip experiment [33]. This case is much closer to the present case, in the sense that the currents in both outgoing channels are noisy by themselves, but their correlations vanish identically due to the cancellation.

Remarkably, the $\mathbb{Z}_2$ peak persists even when the incoming channels are subject to strong inelastic scattering. To model this scenario we employ two voltage probes that are coupled to the two incoming arms, from 1 and 2, respectively [34] (see Fig. 1). For simplicity, we assume the same coupling strength T_p for the two voltage probes. T_p is the probability for electrons in the helical channels to enter the additional reservoir connected by a voltage probe. The vanishing total net currents in the voltage probes require the voltage for both additional reservoirs to be

$$V_p = \frac{2 + (2 - T_p)T + T_p(1 - T_p)T^2}{4 - (T_p T)^2} V_0, \quad (3)$$

where $T = |S_{21}|^2 = |S_{12}|^2$. In the strong coupling limit, $T_p = 1$ and $V_p = V_0/(2 - T)$; the cross correlation P_{34} measures coherent contributions from the two voltage probe reservoirs instead of the original ones 1 and 2. It is clear that the effect of the voltage probes in this limit is only to substitute V_0 in Eq. (2) by V_p. Such a substitution obviously preserves the qualitative structure of the $\mathbb{Z}_2$ peak.

Having established that the suppression of the current cross correlation is a robust feature of TRS-preserving scattering, we now investigate the effect of a weak magnetic field on the present setup. In real experiments, transport measurements on mesoscopic devices normally display sample-dependent fluctuations when varying the magnetic field, due to disorder [35]. In the following, we will include disorder, and, as a consequence, investigate the distribution of the cross-correlation noise power P_{34}. We consider two major effects of the magnetic field in a generic scenario when disorder is included: the first one is the TRS-breaking scattering at the QPC; the second one is the backscattering that may occur along each arm of the helical edge states before approaching the QPC [26]. Here, we generally assume that at small magnetic fields the lengths of the paths between leads and the QPC are smaller than the localization length of the helical edge states [26] such that the current cross correlation is not suppressed simply by localization. We will model the two effects separately, but consistently with scattering theory.

For the TRS-breaking scattering at the QPC, a minimal model requires an additional loop of helical states inserted into the contact area between the two pairs of original edge states (see Fig. 2). This loop is coupled to the original edge states in a pointlike fashion via TRS tunneling. Electrons

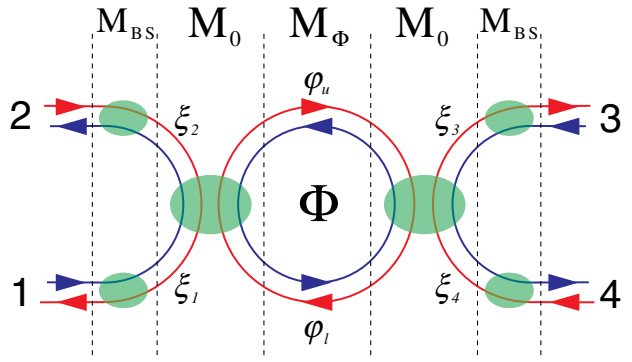

FIG. 2 (color online). Scattering model for the structure shown in Fig. 1 in the presence of a magnetic field and disorder. The setup is partitioned so that the overall scattering matrix can be obtained from combining the transfer matrices (denoted by M). A magnetic field causes a flux Φ in the QPC region and nonzero backscattering along each arm of the helical edge states. Disorder, modeled by random scattering phases ξ_i, φ_u and φ_l as indicated in the figure, leads to a random distribution of the overall scattering matrices.

encircling the loop accumulate an Aharonov-Bohm (AB) phase Φ (cf. Ref. [26]). To obtain a scattering matrix for the combined QPC, we adopt the transfer matrix approach.

The transfer matrix describing the local tunneling between one pair of edge states and the loop states, transformed from a TRS-preserving scattering matrix, is given by

$$M_0 = \frac{1}{\sqrt{1-t^2}}\begin{pmatrix} t\beta\sigma_x & \beta \\ \sigma_x\beta\sigma_x & t\sigma_x\beta \end{pmatrix}, \quad \beta = \frac{1}{\sqrt{1-t^2}}\begin{pmatrix} -s & r \\ r & s \end{pmatrix}, \tag{4}$$

where $t = |S_{12}| = |S_{34}|$, $s = |S_{13}| = |S_{24}|$, and $r = \sqrt{1-t^2-s^2} = |S_{14}| = |S_{23}|$. $\sigma_{i=0,x,y,z}$ are the conventional Pauli matrices. The transfer matrix for the interior of the loop reads

$$M_\Phi = \begin{pmatrix} 0 & \gamma(\Phi) \\ \gamma^*(-\Phi) & 0 \end{pmatrix}, \quad \gamma(\Phi) = \begin{pmatrix} 0 & e^{i(\Phi+\varphi_l)} \\ e^{i\varphi_u} & 0 \end{pmatrix}, \tag{5}$$

where φ_l and φ_u are the dynamic phases for the lower and upper parts of the loop (see Fig. 2). We have chosen a gauge such that the AB phase only enters the lower part of the loop. Transforming the combined transfer matrix $M_{\rm QPC} = M_0 M_\Phi M_0$, we obtain the scattering matrix for the magnetic-flux-dressed QPC,

$$S_{\rm QPC} = \begin{pmatrix} \beta\sigma_x & 0 \\ 0 & \sigma_x\beta \end{pmatrix}\begin{pmatrix} -\Delta_1(\Phi) & \Delta_2(\Phi) \\ \Delta_2^T(-\Phi) & \Delta_1(\Phi) \end{pmatrix}\begin{pmatrix} \beta\sigma_x & 0 \\ 0 & \sigma_x\beta \end{pmatrix}, \tag{6}$$

with $\Delta_1(\Phi) = t\sigma_x[\sigma_0 + \gamma(\Phi)\gamma(-\Phi)]/[\sigma_0 + t^2\gamma(\Phi)\times\gamma(-\Phi)]$ and $\Delta_2(\Phi) = (1-t^2)[\gamma^\dagger(-\Phi) + t^2\gamma(\Phi)]^{-1}$.

In order to illustrate the effect of the magnetic flux on the scattering amplitudes, we extract from Eq. (6) that

$$S_{33}(\Phi) = S_{44}(\Phi) = \frac{rs}{t}\frac{i\sin\Phi}{\cos\Phi + \cos(\varphi - 2i\ln t)}, \tag{7}$$

$$S_{34}(\Phi) = S_{43}(-\Phi) = t\left[1 + \frac{s^2}{t^2 + e^{-i(\varphi+\Phi)}} + \frac{r^2}{t^2 + e^{-i(\varphi-\Phi)}}\right], \tag{8}$$

where $\varphi = \varphi_l + \varphi_u$. Clearly, the backscattering at the QPC is suppressed when $\Phi = 0 \bmod \pi$. On the other hand, by using Eq. (2), we find $P_{34}(\Phi) = P_{34}(-\Phi)$ for the present QPC.

To take into account the backscattering (BS) that occurs along one arm of the helical edge states between a lead and the QPC, we make use of the weak-field-limit result obtained in Ref. [26] and write the scattering matrix as

$$S_{\rm BS}(B) = \begin{pmatrix} -\sqrt{1-\tau(B)^2}e^{i\xi(B)} & \tau(B) \\ \tau(B) & \sqrt{1-\tau(B)^2}e^{-i\xi(B)} \end{pmatrix}, \tag{9}$$

where $\tau(B) = \exp(-\alpha B^2)$ with α being a sample-dependent constant, $\xi(B)$ is a (B-dependent) random phase, and B is the magnetic field. The backscattering can be different for different arms, which again relies on specific disorder configurations, but to include all of them into the full model is straightforward in terms of the transfer matrix approach (see Fig. 2). From this we obtain the full scattering matrix. Details of the above calculation can be found in the Supplemental Material [36].

The full scattering matrix contains parameters that are sample dependent. Varying these parameters allows us to obtain distributions of noise correlations as a function of magnetic field. For simplicity, we fix t, s, and hence r. We also choose a fixed loop area and a fixed α that is the same for all arms. The values of these fixed parameters are determined as described in the Supplemental Material [36] and they permit a sound comparison with numerical simulations that will be presented below. At a specific B, we pick randomly the scattering phases, namely φ_l, φ_u, and ξ's, with a uniform probability distribution in $(0, 2\pi)$. This turns out to be sufficient to produce a random distribution of the full scattering matrix (see below).

The probability distribution of the noise correlation P_{34} produced from the above-described scattering model is plotted in the upper panel of Fig. 3, with the overlaying solid line showing the mean value $\langle P_{34}\rangle$ as a function of B. The $\mathbb{Z}_2$ peak of the noise correlation can be clearly identified either from the probability distribution, or more directly in terms of the mean value. The peak structure extends from weak magnetic field up to the point where the noise correlations are suppressed again due to strong backscattering in individual arms. The maximumly negative

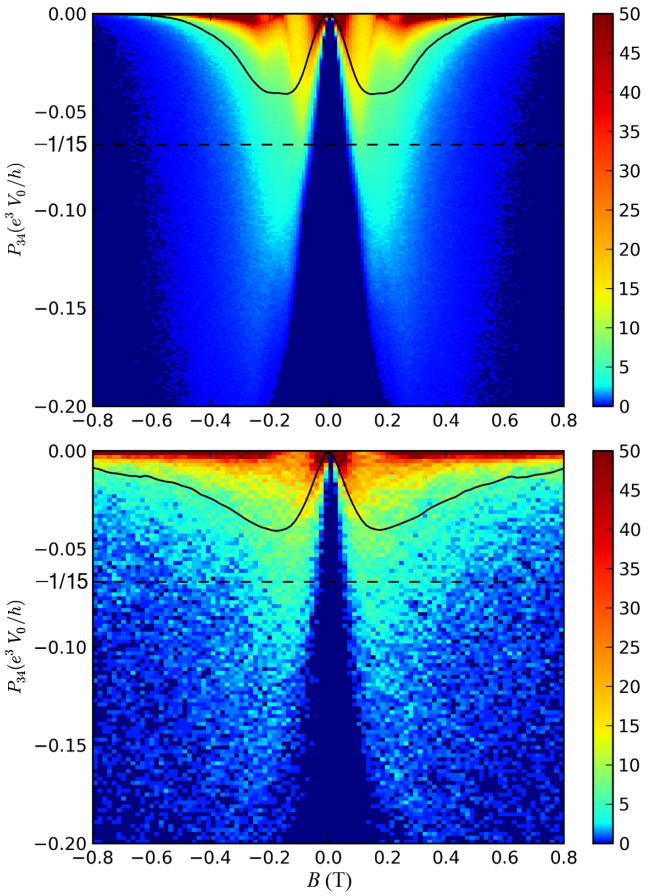

FIG. 3 (color online). Probability distributions of the cross-correlation noise power P_{34} as a function of magnetic field B, obtained from the scattering model with 100 000 disordered samples in the upper panel, and from numerical simulations with 1200 disordered samples in the lower panel. Overlaying both panels, the solid lines show the mean of P_{34}, clearly showing the $\mathbb{Z}_2$ peak at $B = 0$. The dashed lines indicate the average of P_{34} evaluated for a circular unitary ensemble of scattering matrices.

value of $\langle P_{34}(B)\rangle$ is compared with the average of P_{34} for the circular unitary ensemble of four-by-four scattering matrices, given by the dashed line. The circular unitary ensemble (CUE) contains uniformly distributed unitary matrices to which the TRS-breaking scattering matrices belong [37]. Averaging Eq. (2) in this ensemble yields $\langle P_{34}\rangle_{\mathrm{CUE}} = -(1/15)e^3V_0/h$. The maximumly negative value of $\langle P_{34}(B)\rangle$ approaches, but does not reach, $\langle P_{34}\rangle_{\mathrm{CUE}}$. This, on the one hand, justifies that by only varying the scattering phases a reasonably random distribution of scattering matrices can be obtained. On the other hand, it also indicates that this random distribution is not quite uniform.

To examine the validity of our scattering model, we further perform numerical simulations with a microscopic Hamiltonian (see Supplemental Material [36] for details). We construct numerically a device as illustrated in Fig. 1 from a lattice model of the HgTe/CdTe quantum wells [4], described at low energy by the Bernevig-Hughes-Zhang Hamiltonian [6]. Disorder is introduced by adding random on-site potentials of a Gaussian profile. The resulting potential fluctuation has a magnitude smaller than the bulk band gap and a correlation length comparable to the penetration depth of the edge states. Scattering matrices connecting transmitting modes between leads are computed from Green's functions [38] at various magnetic fields for each disorder configuration. The probability distribution of the noise correlation P_{34} is then obtained by using Eq. (2), and plotted in the lower panel of Fig. 3. Comparing with the upper panel, we observe a remarkable agreement between the numerical simulation and the scattering model at weak field, despite a minor quantitative disagreement at stronger field since our choice of $S_{BS}(B)$ in Eq. (9) is no longer valid.

To summarize, we have constructed a model for a QPC in a QSH system in the presence of disorder, subject to a magnetic field. We have computed the ensemble properties of the noise correlations for this model and found a favorable comparison with results from a numerical calculation. In particular, both approaches show the presence of the $\mathbb{Z}_2$ peak, a maximum of the noise correlations at zero magnetic field.

We acknowledge useful discussions with C. W. J. Beenakker and T. Schmidt, and helpful comments from Patrick Hofer and Michael Moskalets. This research was supported by NanoCTM, nanoICT, Swiss NSF, MaNEP, and QSIT. J. M. E. and J. L. contributed equally to this work.

[1] Y. M. Blanter and M. Büttiker, Phys. Rep. **336**, 1 (2000).
[2] P. Samuelsson, E. V. Sukhorukov, and M. Büttiker, Phys. Rev. Lett. **92**, 026805 (2004).
[3] I. Neder, N. Ofek, Y. Chung, M. Heiblum, D. Mahalu, and V. Umansky, Nature (London) **448**, 333 (2007).
[4] M. König, S. Wiedmann, C. Brüne, A. Roth, H. Buhmann, L. W. Molenkamp, X.-L. Qi, and S.-C. Zhang, Science **318**, 766 (2007).
[5] C. L. Kane and E. J. Mele, Phys. Rev. Lett. **95**, 226801 (2005).
[6] B. A. Bernevig, T. L. Hughes, and S.-C. Zhang, Science **314**, 1757 (2006).
[7] A. Roth, C. Brüne, H. Buhmann, L. W. Molenkamp, J. Maciejko, X.-L. Qi, and S.-C. Zhang, Science **325**, 294 (2009).
[8] C. Brüne, A. Roth, H. Buhmann, E. M. Hankiewicz, L. W. Molenkamp, J. Maciejko, X.-L. Qi, and S.-C. Zhang, Nat. Phys. **8**, 486 (2012).
[9] M. König, M. Baenninger, A. G. F. Garcia, N. Harjee, B. L. Pruitt, C. Ames, P. Leubner, C. Brüne, H. Buhmann, L. W. Molenkamp, and D. Goldhaber-Gordon, Phys. Rev. X **3**, 021003 (2013).
[10] K. C. Nowack, E. M. Spanton, M. Baenninger, M. König, J. R. Kirtley, B. Kalisky, C. Ames, P. Leubner, C. Brüne,

H. Buhmann, L. W. Molenkamp, D. Goldhaber-Gordon, and K. A. Moler, arXiv:1212.2203.
[11] Y. Ma, W. Kundhikanjana, J. Wang, M. R. Calvo, B. Lian, Y. Yang, K. Lai, M. Baenninger, M. König, C. Ames, C. Brüne, H. Buhmann, P. Leubner, Q. Tang, K. Zhang, X. Li, L. W. Molenkamp, S.-C. Zhang, D. Goldhaber-Gordon, M. A. Kelly, and Z.-X. Shen, arXiv:1212.6441.
[12] J. I. Väyrynen, M. Goldstein, and L. I. Glazman, Phys. Rev. Lett. **110**, 216402 (2013).
[13] M. Reznikov, M. Heiblum, H. Shtrikman, and D. Mahalu, Phys. Rev. Lett. **75**, 3340 (1995).
[14] A. Kumar, L. Saminadayar, D. C. Glattli, Y. Jin, and B. Etienne, Phys. Rev. Lett. **76**, 2778 (1996).
[15] C.-Y. Hou, E.-A. Kim, and C. Chamon, Phys. Rev. Lett. **102**, 076602 (2009).
[16] J. C. Y. Teo and C. L. Kane, Phys. Rev. B **79**, 235321 (2009).
[17] G. Dolcetto, S. Barbarino, D. Ferraro, N. Magnoli, and M. Sassetti, Phys. Rev. B **85**, 195138 (2012).
[18] A. Ström and H. Johannesson, Phys. Rev. Lett. **102**, 096806 (2009).
[19] J.-R. Souquet and P. Simon, Phys. Rev. B **86**, 161410 (2012).
[20] Y.-W. Lee, Y.-L. Lee, and C.-H. Chung, Phys. Rev. B **86**, 235121 (2012).
[21] T. L. Schmidt, Phys. Rev. Lett. **107**, 096602 (2011).
[22] M. Büttiker, Phys. Rev. B **46**, 12485 (1992).
[23] C. Xu and J. E. Moore, Phys. Rev. B **73**, 045322 (2006).
[24] C. Wu, B. A. Bernevig, and S. C. Zhang, Phys. Rev. Lett. **96**, 106401 (2006).
[25] N. Lezmy, Y. Oreg, and M. Berkooz, Phys. Rev. B **85**, 235304 (2012).
[26] P. Delplace, J. Li, and M. Büttiker, Phys. Rev. Lett. **109**, 246803 (2012).
[27] V. Krueckl and K. Richter, Phys. Rev. Lett. **107**, 086803 (2011).
[28] J. Splettstoesser, M. Moskalets, and M. Büttiker, Phys. Rev. Lett. **103**, 076804 (2009).
[29] On the other hand, if the spin-flip scattering process, such as represented by S_{13}, were absent, P_{34} would trivially be zero.
[30] M. Henny, S. Oberholzer, C. Strunk, T. Heinzel, K. Ensslin, M. Holland, and C. Schönenberger, Science **284**, 296 (1999).
[31] S. Oberholzer, M. Henny, C. Strunk, C. Schönenberger, T. Heinzel, K. Ensslin, and M. Holland, Physica (Amsterdam) **6E**, 314 (2000).
[32] S. Olkhovskaya, J. Splettstoesser, M. Moskalets, and M. Büttiker, Phys. Rev. Lett. **101**, 166802 (2008).
[33] E. Bocquillon, V. Freulon, J.-M. Berroir, P. Degiovanni, B. Plaçais, A. Cavanna, Y. Jin, and G. Fève, Science **339**, 1054 (2013).
[34] M. Büttiker, IBM J. Res. Dev. **32**, 63 (1988).
[35] S. Washburn and R. A. Webb, Adv. Phys. **35**, 375 (1986).
[36] See Supplemental Material at http://link.aps.org/supplemental/10.1103/PhysRevLett.110.246601 for details of the derivation of the transfer matrices and the numerical calculation in terms of recursive Green's functions.
[37] C. W. J. Beenakker, Rev. Mod. Phys. **69**, 731 (1997).
[38] D. S. Fisher and P. A. Lee, Phys. Rev. B **23**, 6851 (1981).